Journal of Power Sources 262 (2014) 407–413

Contents lists available at ScienceDirect

Journal of Power Sources

journal homepage: www.elsevier.com/locate/jpowsour

Zirconium phosphate reinforced short side chain perflurosulfonic acid membranes for medium temperature proton exchange membrane fuel cell application

Mario Casciola [a,*], Paula Cojocaru [b], Anna Donnadio [a,1], Stefano Giancola [a,3], Luca Merlo [b], Yannig Nedellec [c], Monica Pica [a,2], Surya Subianto [c]

[a] Department of Chemistry, via Elce di Sotto 8, 06123 Perugia, Italy
[b] Solvay Specialty Polymers, viale Lombardia 20, 20021 Bollate, MI, Italy
[c] Institute Charles Gerhardt, Equipe AIME, Université Montpellier 2, France

HIGHLIGHTS

- 30 μm thick SSC PFSA membranes filled with nanosized zirconium phosphate (ZrP).
- Composite membranes as conductive as the neat PFSA ionomer.
- Overall improvement of membrane mechanical properties with increasing ZrP loading.
- Fuel cell performance of the composites better than that of neat ionomer at 110 °C.

ARTICLE INFO

Article history:
Received 18 December 2013
Received in revised form
5 March 2014
Accepted 3 April 2014
Available online 13 April 2014

Keywords:
Perflurosulfonic acid
Short side chain ionomer
Mechanical properties
Proton conductivity
Water uptake
Fuel cell tests

ABSTRACT

Composite membranes, made of an 830 equivalent weight short-side-chain perfluorosulfonic acid ionomer and containing up to 10 wt% zirconium phosphate (ZrP), are prepared by casting dispersions of ZrP nanoparticles in the ionomer solution. 30 μm thick composite membranes are characterized by transmission electron microscopy, X-ray diffraction, stress–strain tests, conductivity measurements, water uptake and ion-exchange capacity determinations, as well as fuel cell tests in H_2/air. In comparison with the neat ionomer, the tensile modulus (E) and the yield stress (Y) of the composite membranes increase with the ZrP content, both at room temperature ($\Delta E/E$ up to +75%, $\Delta Y/Y$ up to +47%) and at 80 °C/70% relative humidity ($\Delta E/E$ up to +64%, $\Delta Y/Y$ up to +103%). Despite their lower hydration, the composite membranes are as conductive as the neat ionomer and the in-plane conductivity at 110 °C ranges from ~0.005 S cm^{-1} at 25% RH to 0.14 S cm^{-1} at 90% RH. The fuel cell performance of a catalyst coated membrane loaded with 10 wt% ZrP is weakly affected by temperature in the range 80–110 °C. The peak power density decreases from 0.36 W cm^{-2}, at 80 °C, to 0.28 W cm^{-2} at 110 °C, where the composite membrane performs better than the neat ionomer.

1. Introduction

The combination of the properties of polytetrafluoroethylene with those of the strongly acidic sulfonic group in the same macromolecule paved the way, in the 60s, for the development of the most famous class of ionomers, generally known as perfluorosulfonic acid (PFSA) ionomers [1]. PFSA membranes have been widely employed as electrolytes in electrochemical devices such as proton exchange membrane fuel cells (PEMFCs), since they represent the best compromise between chemical stability and high proton conductivity, in spite of their relatively low mechanical stability if compared with non-fluorinated ionomers [2].

* Corresponding author. Present address: Department of Chemistry, Biology and Biotechnologies, via Elce di Sotto 8, 06123 Perugia, Italy. Tel.: +39 075 5855567; fax: +39 075 5855566.
E-mail address: mario.casciola@unipg.it (M. Casciola).
[1] Present address: Department of Chemistry, Biology and Biotechnologies, via Elce di Sotto 8, 06123 Perugia, Italy.
[2] Present address: Department of Pharmaceutical Sciences, via del Liceo 1, 06123 Perugia, Italy.
[3] Present address: Institute Charles Gerhardt, Equipe AIME, Université Montpellier 2, France.

http://dx.doi.org/10.1016/j.jpowsour.2014.04.010
0378-7753/

The properties of PFSA ionomers can be tuned by varying both the equivalent weight (EW) and the length of the side chains bearing the sulfonic groups. On this regards, PFSAs can be classified as long side chain (LSC) and short side chain (SSC) ionomers. In the SSC ionomer commercially available with the name of Aquivion® the side chain consists of two $-CF_2-$ groups bearing the sulfonic group at one end and bonded to the ionomer main chain through an oxygen atom at the other end. This kind of SSC ionomers exhibit higher crystallinity at a given equivalent weight (EW) compared to LSC ionomers [3–5]. For example, it has been demonstrated that an 850 EW SSC ionomer shows a degree of crystallinity similar to that of 1100 EW Nafion, which returns in similar mechanical properties, associated to a higher membrane conductivity of the SSC ionomer with respect to the LSC one [5].

Ionomeric membranes, suitable for application in PEMFCs, should exhibit low area specific resistance which can be achieved by reducing the membrane thickness to around 25–30 μm, with a negative impact on the membrane strength. In a recent work, the mechanical properties of 100 μm thick SSC ionomer membranes were successfully improved by incorporating, within the polymer matrix, layered zirconium phosphate (ZrP) nanoparticles [6]. ZrP was chosen as inorganic filler since it associates chemical and thermal stability with intrinsic good proton conductivity. Moreover, ZrP was already employed as a filler in Nafion membranes and turned out to be able to effectively reinforce the ionomer matrix [7–16].

In the present paper, a similar strategy was employed in order to mechanically reinforce thin SSC ionomer membranes. With this aim, 30 μm thick membranes based on an 830 EW SSC ionomer incorporating 5 and 10 wt% ZrP nanoparticles (hereafter C83/ZrP-5 and C83/ZrP-10, respectively) were prepared by solution casting and characterised by mechanical stress–strain tests, conductivity measurements and water uptake determinations under controlled temperature and relative humidity (RH) conditions, as well as by fuel cell tests in H_2/air up to 110 °C. The physicochemical properties of the composite membranes are compared with those of the neat 830 EW SSC ionomer membrane obtained by casting (hereafter C83) and with those of an extruded 790 EW SSC ionomer membrane (hereafter E79) of the same thickness.

2. Experimental

2.1. Chemicals

A 24 wt% Aquivion® dispersion in water (D83-24B, EW = 830 g/eq) and the E79 extruded membrane (Aquivion®, 30 μm thick) were supplied by Solvay Specialty Polymers, Italy. Zirconyl propionate ($ZrO_{1.26}(C_2H_5COO)_{1.49}$, MW = 220 Da) was supplied by MEL Chemicals, England. Concentrated orthophosphoric acid (85%, 14.8 M) was supplied by Fluka. Anhydrous propanol was purchased from Carlo Erba. All other reagents were purchased by Aldrich.

2.2. Preparation of neat ionomer membranes

10 mL of propanol were added to 4.16 g of the ionomer dispersion in water. After stirring at room temperature for 2 h, the mixture was cast on a glass Petri dish and put in oven at 80 °C for 2 h in order to remove the solvent. The obtained membrane was re-dissolved in 20 mL propanol under stirring at room temperature and then recast on a glass support by an Elcometer Doctor Blade Film Applicator 4340 with transverse speed of 2 mm min^{-1} and bar height of 500 μm. After heating in an oven at 80 °C for 2 h to remove the solvent, the membrane was detached from the glass and annealed at 190 °C for 30 min. Finally, the membrane was treated, at room temperature, according to the following procedure: 15 h in 1 M HCl solution, 1 h in deionised water, 2 h in 3% vol H_2O_2 solution, 1 h in deionised water. This kind of membrane, about 30 μm thick, will be hereafter indicated as C83.

2.3. Preparation of composite membranes containing ZrP nanoparticles

A gel of ZrP particles in propanol, containing about 10 wt% ZrP, was prepared according to ref. 17. For the preparation of composite membranes containing 5 and 10 wt% ZrP, a weighed amount of the ZrP gel was diluted with 10 mL of propanol and left under stirring for 2 h. The diluted gel was mixed with 4.5 g of the ionomer dispersion in water and the mixture was stirred for 2 h before casting and solvent evaporation (80 °C for 2 h). The membrane thus obtained was re-dissolved in 20 mL propanol under stirring at room temperature and then recast and treated as described in the previous section. The resulting composite membrane (hereafter C83/ZrP-x, where x represents the ZrP wt%) was about 30 μm thick.

2.4. Techniques

X-ray powder diffraction (XRD) patterns were collected with a Panalytical X'Pert PRO diffractometer and a PW3050 goniometer equipped with an X'Celerator detector using the Cu Kα radiation source with a 2θ step size of 0.0170 and step scan of 20 s. The LFF ceramic tube was operated at 40 kV, 40 mA. According to Fujimura [18], the ionomer peak at ~17° 2θ was deconvoluted into the crystalline and amorphous components with the programme XFIT by using pseudo Voigt functions.

Transmission electron microscopy (TEM) analysis was carried out by a JEOL 1200 EXII microscope operating at 120 kV. The samples were embedded in an epoxy resin and dried at 80 °C for 24 h. Microtomed sections of 70–90 nm thickness were prepared using a Reichert ultramicrotome and deposited on copper grids (Agar).

Stress–strain mechanical tests were carried out by a Zwick Roell Z1.0 testing machine, with a 200 N static load cell, equipped with a climatic chamber operating in the RH range 30–95% (±0.5%) and in the temperature range from room temperature to 80 °C (±0.5 °C). Young's modulus (the slope of the stress–strain curve in the elastic deformation region), yield stress (maximum stress that can be developed without causing plastic deformation) and elongation at break (the percentage increase in length that occurs before the sample breaks) were measured on rectangle shaped film stripes, length and width of which were 100 and 5 mm, respectively. Before the tests at room temperature, samples were equilibrated for 7 days in vacuum desiccators at 53% RH and room temperature (20–23 °C). The high temperature tests were performed after equilibration of the samples in the climate chamber at 80 °C and 70% relative humidity for one day. The thickness of the film stripe, determined with an uncertainty of 5 μm, was in the range 25–30 μm. An initial grip separation of 10,000 ± 0.002 mm and a crosshead speed of 30 mm min^{-1} were used. At least five replicate film stripes were analysed. The area under the stress–strain curves was used to calculate the modulus of toughness, which is a measure of the energy that a sample can absorb before it breaks.

The in-plane conductivity of the membranes was determined on (5 cm × 0.5 cm) membrane strips in the frequency range 10 Hz–100 kHz, at 100 mV signal amplitude, by four-probe impedance measurements using an Autolab, PGSTAT30 potentiostat/galvanostat equipped with an FRA module as described in Ref. [19].

The through-plane conductivity was measured on 5 staged membrane discs, 8 mm in diameter, sandwiched between gas diffusion electrodes (ELAT containing 1 mg cm^{-2} Pt loading) which were pressed on the membranes by means of porous stainless steel

discs with an initial applied pressure of 20 kg cm^{-2}. Impedance measurements were carried out by an HP4192A Impedance Analyser in the frequency range 100 Hz–1 MHz at a signal amplitude ≤100 mV. The impedance data were corrected for the contribution of the empty and short-circuited cell. The membrane resistance was obtained by extrapolating the impedance data to the real axis on the high frequency side.

For both in-plane and through-plane measurements RH was controlled by using stainless steel sealed-off cells consisting of two communicating cylindrical compartments held at different temperatures. The cold compartment contained water, while the hot compartment housed the membrane under test. RH values were calculated from the ratio between the pressures of saturated water vapour (p) at the temperatures of the cold (Tc) and hot (Th) compartment: $RH = p(Tc)/p(Th) \times 100$.

Water uptake (WU) at controlled temperature and RH was determined as described in Ref. [19]. Specifically, the cell for water uptake has the same size and shape as the conductivity cell and differs from that mainly because the membrane electrode assembly (MEA) holder is replaced by a glass container hosting the membrane sample (≈0.5 g). The cell is equipped with a device which allows to close the sample container with a teflon plug without opening the cell. After a suitable equilibration time (usually a day) at the desired temperature and RH, the sample container is closed, extracted from the cell and weighed. The water content (λ, number of water molecules per sulfonic group) is determined on the basis of the weight of the membrane dried at 130 °C taking into account the amount of water trapped in the sample container at the temperature and RH of the experiment. The error on the determination of λ is estimated to be ±0.5 at most.

The ion-exchange capacity (IEC) of the membranes was determined by acid–base titrations with a Radiometer automatic titrimeter (TIM900 TitraLab and ABU91 Burette) operating at the equilibrium point method. Before titration, the membranes were heated at 120 °C for 3 h in order to eliminate water and to determine the weight of the anhydrous sample. The dry membranes were equilibrated overnight, at room temperature, with a 0.1 M NaCl aqueous solution in order to exchange Na^+ ions for the membrane protons. The solutions were then titrated with 0.1 M NaOH without removing the membranes.

2.5. Fuel cell tests

Fuel cell tests were carried out with MEAs using gas diffusion electrodes (GDEs) or with MEAs made of a catalyst coated membrane (CCM). In the GDE (supplied by Johnson Matthey Fuel Cells) the gas diffusion layer was carbon paper and the catalyst layer used Nafion as the ionomer with catalyst loading of 0.2 mg cm^{-2} on the anode and 0.4 mg cm^{-2} on the cathode, and the MEA was made by hot-pressing the GDE onto the membrane at 150 °C for 3 min.

In the CCM-type MEA the membrane was coated by the catalyst via the DECAL method by using the D83-24B ionomer dispersion and a TANAKA catalyst (0.25 mg cm^{-2} Pt, 50%Pt/C for both cathode and anode). The catalyst was transferred to the membrane by applying 1.5 bar pressure for 3 min, at 180 °C. The CCM was then incorporated without hot-pressing into the MEA using a Sigracet 10BC gas diffusion layer with a microporous layer on one side.

The MEA was then incorporated in the fuel cell setup using Fluorinated Ethylene Propylene (FEP) gaskets at 15% compression, mounted on a Lynntech Fuel Cell Test system equipped with a flash evaporator. A MEA break-in step of 14 h at 0.5 A cm^{-2} at 80 °C and 100%RH under H_2/Air (using a 1.5/2 stoichiometry of H_2/O_2) was performed prior to the actual tests. The polarisation curves were collected after 6 h of equilibration at 0.5 A cm^{-2} under the appropriate temperature and RH by setting the cell current density at predetermined points and holding the current density for 3 min at each point. Tests at low humidity were performed under a back pressure of 0.5 bar (1.5 bar absolute pressure) by regulating the back pressure before equilibration and before each 3-min holding step during the polarisation curve.

3. Results and discussion

Fig. 1 shows the TEM image of a C83/ZrP-10 membrane. The filler particles consist of nanosheets, with homogeneous planar size of 40–50 nm and aspect ratio of about 10, which are fairly uniformly distributed within the polymer matrix. A similar morphology and size distribution was also observed for the ZrP particles of the gel employed for the preparation of the composites [17], thus indicating that the filler particles kept their size and morphology substantially unchanged after incorporation within the polymer matrix.

Fig. 2 shows the X-ray diffraction patterns of the composites containing 5 and 10 wt% ZrP, together with the pattern of a C83 sample. It is noteworthy that even with 10 wt% filler loading, the typical reflections of ZrP (at 11.7°, 19.8°, 24.9°, 33.8° 2θ) are not observed in the pattern of the composites, indicating that the filler is highly exfoliated within the polymer matrix, in agreement with TEM analysis. Moreover, the area of the broad peak of the ionomer, centred at $2\theta \approx 17°$, decreases by 13 and 30% for 5 and 10 wt% ZrP loading, respectively. This reduction is greater than that expected on the basis of the ionomer mass fraction and according to Ref. [20] it can be partially attributed to electron dense Zr(IV) scattering centers shielding the interior of the polymer membrane.

The deconvolution of the ionomer peak into the components associated with the crystalline and amorphous parts of the ionomer shows that the area of both components, similarly to the overall peak area, decreases with increasing filler loading and that these changes are more relevant for the crystalline component. As a consequence, the ratio between the area of the crystalline component and the area of the amorphous component decreases from 0.26 in C83 to 0.20 and 0.19 in C83/ZrP-5 and C83/ZrP-10, respectively, thus indicating that the filler makes the ionomer less crystalline.

3.1. Mechanical properties

The mechanical properties of a cast C83 membrane were determined by stress–strain tests, under controlled conditions of temperature and relative humidity. For each test, the stress–strain curve with the greatest elongation at break was chosen since it is representative of the specimen with less macroscopic defects. Fig. 3

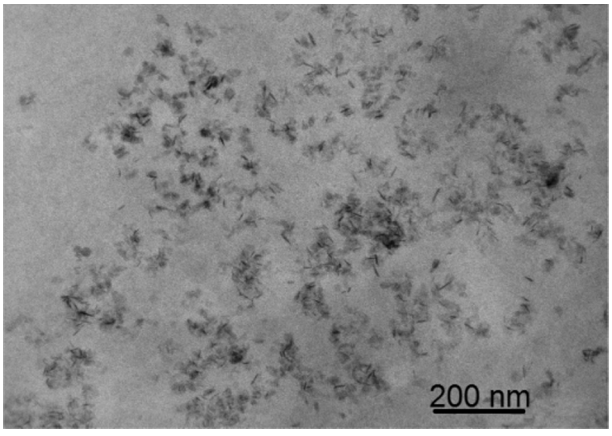

Fig. 1. TEM picture of a C83/ZrP-10 composite membrane.

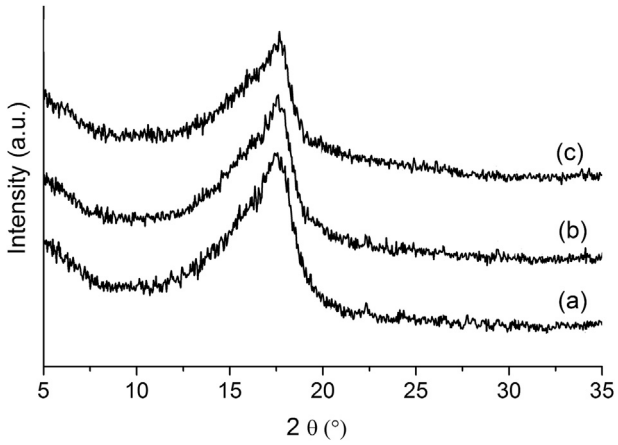

Fig. 2. X-ray diffraction patterns of (a) C83, (b) C83/ZrP-5 and (c) C83/ZrP-10.

shows the stress–strain curve obtained at 20 °C and 53% RH. The membrane exhibits the typical behaviour of ductile polymers: after reaching the yield point, the stress first drops slightly and then gradually increases with strain (strain hardening).

In order to improve the mechanical resistance of neat C83 membranes, nanosized ZrP particles were incorporated within the polymer matrix. The stress–strain curves of the composite membranes, collected at 20 °C and 53% RH, are compared with that of C83 in Fig. 3. The mechanical parameters derived from the stress–strain curves are listed in Table 1. While the presence of the filler does not modify the profile of the stress-strain curve of neat C83, the composites display an enhanced mechanical strength associated with a reduced elongation at break. In particular, a 10 wt% filler loading increases the yield stress and the Young's modulus by 47% and 75%, respectively. In all cases, the elongation at break is ≥84% and, at this elongation, the modulus of toughness of the composites is significantly higher (1041 MPa for 5 wt% ZrP and 1207 MPa for 10 wt% ZrP) than that of C83 (828 MPa). These findings prove that the filler effectively acts as a stiffener of the polymer matrix, which however keeps a good plastic behaviour.

The mechanical properties of the extruded E79 membrane were also investigated at 20 °C and 53% RH. The stress strain curve of this membrane lies between the curve of C83 and that of C83/ZrP-5. In comparison with C83, E79 shows a slightly lower Young's modulus

Table 1
Mechanical properties at different temperature and RH values for C83, E79 and C83/ZrP membranes.

Membrane	T (°C)/%RH	Young's modulus (MPa)	Yield stress (MPa)	Elongation at break (%)
E79	20/53	149 ± 8	11.8 ± 0.6	198
C83	20/53	183 ± 10	9.7 ± 0.5	174
C83/ZrP-5	20/53	253 ± 19	12.2 ± 0.7	153
C83/ZrP-10	20/53	321 ± 19	14.2 ± 0.8	84
C83	80/70	72 ± 17	4.0 ± 0.9	126
C83/ZrP-10	80/70	118 ± 13	7.7 ± 1.0	66

(Table 1) but a higher yield point followed by larger strain hardening and elongation at break.

The stress–strain curves of C83 and C83/ZrP-10 membranes were also collected at 80 °C–70% RH. In both cases, the simultaneous increase in temperature and RH resulted in a strong decrease in the Young's modulus, in the yield stress and, to a lesser extent, in the elongation at break (Table 1). Nevertheless, the composite membrane is still significantly more robust than C83 (+64% for the Young's modulus and +103% for the yield stress).

Comparison between the mechanical parameters of Table 1 with those previously reported for "thick" C83/ZrP composite membranes shows that the Young's modulus of the membranes here investigated is, on average, higher by about 40% than that of the "thick" membranes [6], while the two membrane types have similar yield stress values.

3.2. Proton conductivity

The in-plane conductivity (σ) of neat and composite C83 membranes was determined at 110 °C as a function of RH. The membranes were first conditioned overnight at 110 °C–25% RH in the conductivity cell and then measurements were performed at increasing RH up to 90%. Fig. 4 shows that σ is nearly independent of filler loading but strongly influenced by changes in RH going from values around 0.005 S cm^{-1} at 25% RH to values above 0.1 S cm^{-1} at 90% RH. Under the same conditions, E79 is more conductive than neat and composite C83 membranes by an average factor of 1.8. The fact that this value is significantly higher than the reciprocal ratio of the ionomer equivalent weights (i.e 1.05) suggests that, besides proton concentration, the membrane conductivity is also strongly affected by the ionomer morphology (in terms of connectivity and/or tortuosity and/or orientation of the

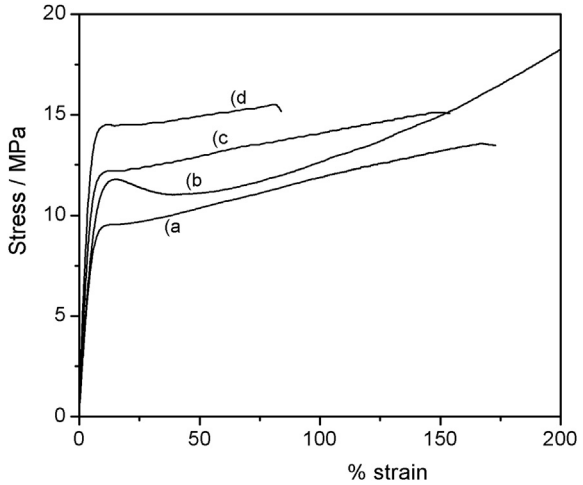

Fig. 3. Stress–strain curves at 20 °C for (a) C83, (b) E79, (c) C83/ZrP-5 and (d) C83/ZrP-10 membranes.

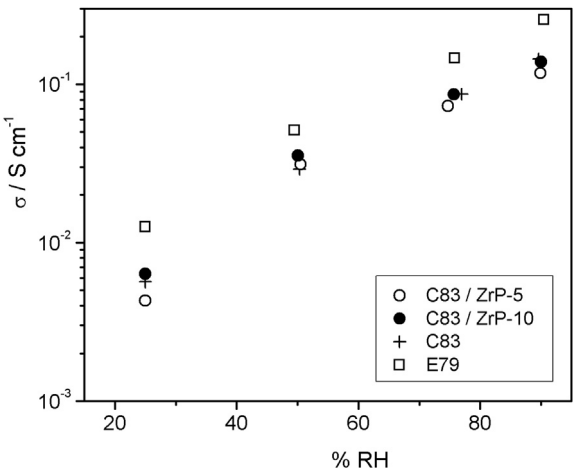

Fig. 4. In-plane conductivity at 110 °C as a function of RH for neat C83 and E79 membranes and for C83/ZrP composite membranes.

Table 2
Hydration (λ) at 110 °C for E79, C83 and C83/ZrP-10 membranes as a function of RH.

% RH	$\lambda \pm 0.5$		
	E79	C83	C83/ZrP-10
25	4.1	3.9	3.6
50	5.4	5.0	4.7
75	8.4	8.0	6.4
90	13.2	11.0	9.4

conduction pathways) determined by the different membrane fabrication process.

Taking into account that C83/ZrP-10 is the most robust membrane and is as conductive as C83/ZrP-5, it was further investigated together with E79 and C83 to get an insight into the factors affecting the membrane conductivity. The IEC values of E79 (1.21 meq g^{-1}) and C83 (1.10 meq g^{-1}) were slightly lower than those calculated from their nominal equivalent weights, while the IEC value of the composite membrane (1.32 meq g^{-1}) was higher than that of C83 due to the presence of ZrP (IEC = 6.64 meq g^{-1}). On the basis of the difference between the IEC of the composite membrane and that of C83, the effective IEC of ZrP turns out to be 3.3 meq g^{-1} which just half of the expected IEC value. Similar results were also reported for Nafion membranes filled with ZrP [12,21,22]. These findings can be explained on the basis of the ion exchange behavior of microcrystalline ZrP [23]. The replacement of the protons of the two monohydrogen phosphate groups with sodium ions occurs in two steps: in the first step half of the protons are exchanged with formation of $Zr(HPO_4)(NaPO_4)$, which is converted into $Zr(NaPO_4)_2$ in the second step. During each step the exchange process proceeds at nearly constant pH and, independent of the Na^+ concentration, the pH of the second step is by three units higher than the pH of the first step. In other words, protons are more easily exchanged in the first step than in the second step and this is likely the reason why only half of the protons are exchanged when ZrP is embedded in the ionomer matrix.

WU determinations were carried out at 110 °C under the same RH conditions employed for the conductivity measurements and the WU values were used to calculate the number of water molecules per sulfonic group (λ) for E79 and C83. The same calculation was also made for the composite membrane after subtraction of the ZrP water content from the overall membrane WU by assuming that ZrP is monohydrated over the investigated RH range [24]. This implies that the water content of the filler is about 0.7% of the weight of the anhydrous composite membrane, being therefore a small fraction of the overall membrane WU which ranges from 7.1 wt% at 25% RH to 17.5% wt% at 90% RH.

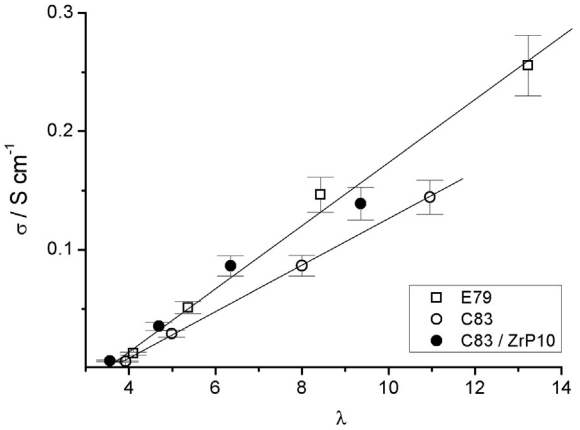

Fig. 5. In-plane conductivity, at 110 °C, as a function of hydration for E79, C83 and C83/ZrP-10.

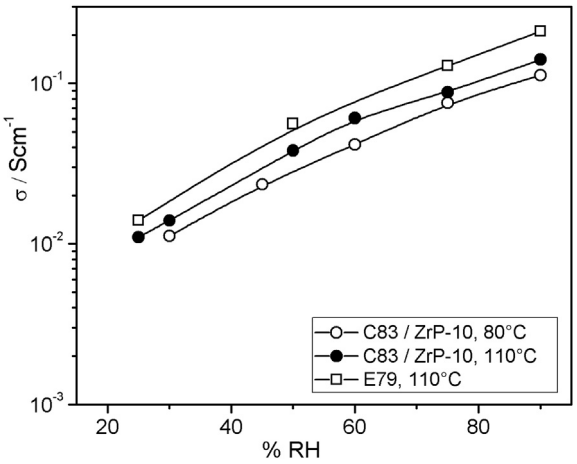

Fig. 6. Through-plane conductivity as a function of RH for C83/ZrP-10 and E79 membranes.

The λ values for E79, C83 and C83/ZrP-10 are listed in Table 2. At low RH all three membranes have similar λ values but with increasing RH the λ sequence

$$E79 > C83 > C83/ZrP - 10$$

becomes progressively more evident. These findings are consistent with the mechanical properties of the membrane, because the ionomer water content depends on the counter-elastic force acting on the aqueous nanofase [25]: the weaker the Young's modulus, the larger the ionomer hydration. The influence of counter-elastic force on the ionomer hydration is stronger for weakly bonded than for strongly bonded water, which explains why the composite membrane becomes progressively less hydrated than the neat ionomer with increasing RH.

From Fig. 4 and Table 2 it is seen that, at the same RH, C83 and C83/ZrP-10 have the same conductivity although the composite membrane is less hydrated than C83. Therefore, in order to highlight the conductivity dependence on hydration, the conductivity of the three membranes was plotted as a function of λ. Fig. 5 shows that in the investigated RH range the membrane conductivity

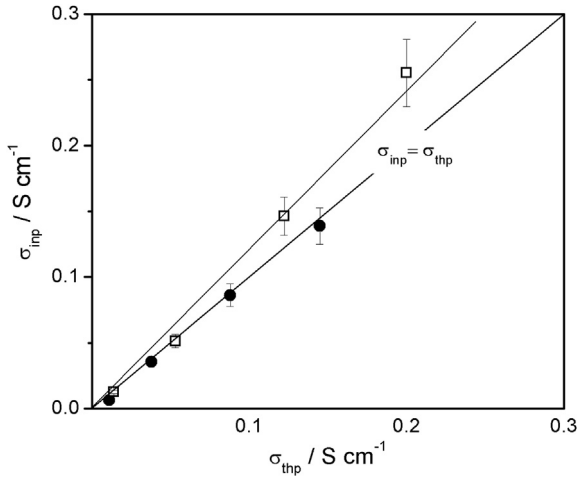

Fig. 7. Comparison between in-plane and through-plane conductivity at 110 °C for C83/ZrP-10 and E79 membranes.

depends linearly on λ and that the points representing E79 and C83/ZrP-10 gather around the same straight line, while those representing C83 lie on a different straight line with lower slope. Therefore, the ionomer hydration being the same, the presence of the filler makes the composite membrane as conductive as E79 and more conductive than C83. Since the filler is less conductive than the ionomer (at 100 °C and 90% RH the conductivity of nanosized ZrP is of the order of 0.01 S cm^{-1}), we suggest that the higher conductivity of the composite membrane arises from structural changes of the ionomer matrix induced by the presence of the filler. This suggestion is supported by the analysis of the X-ray data (showing a decreased ionomer crystallinity in the presence of the filler) and by the slightly lower density of anhydrous C83/ZrP-10 (1.8 ± 0.06 g cm^{-3}) in comparison with the density of anhydrous C83 (2.0 ± 0.07 g cm^{-3}). Actually, since ZrP has higher density (2.72 g cm^{-3} [23]) than C83, the lower density of the composite membrane must be ascribed to a less dense ionomer structure. Similar results were also reported for Nafion/ZrP composite membranes [21].

C83/ZrP-10 was further investigated by through-plane conductivity measurements as a function of RH, at 80 and 110 °C. The through-plane conductivity shows substantially the same dependence on RH at both temperatures and is weakly dependent on temperature, the conductivity at 110 °C being on average higher than that at 80 °C by a factor of 1.3 (Fig. 6). As already observed for the in-plane conductivity, the C83/ZrP-10 through-plane conductivity as well is lower than that of the extruded E79 membrane.

Comparison between Figs. 4 and 6 shows however that the difference in conductivity between E79 and the composite membrane is larger for the in-plane conductivity, thus indicating that proton transport has a different anisotropic character in the two membrane types. It was therefore of interest to compare directly through-plane (σ_{thp}) and in-plane (σ_{inp}) conductivity by plotting σ_{inp} as a function of σ_{thp}. Fig. 7 shows that while the points representing C83/ZrP-10 lie on the diagonal of the plot ($\sigma_{inp} = \sigma_{thp}$), those representing E79 gather around a straight line with slope greater than 1. The conductivity is highly isotropic in the composite membrane and anisotropic in E79, probably due to the fact that, in comparison with casting, the extrusion process favours to a larger extent preferred orientation of the polymer chains along the membrane surface.

3.3. Fuel cell tests

Preliminary fuel cell tests were carried out at 80 °C with 30% RH both at the anode and the cathode on GDE or CCM type MEAs. Fig. 8a shows the polarisation curves obtained for GDE MEAs based on C83/ZrP-10, C83 and extruded E79 membranes. While C83 and E79 exhibit similar *I–V* curves, the performance of the composite membrane is much worse: starting from an OCV value of about 900 mV, the potential drops suddenly by more than 300 mV as soon

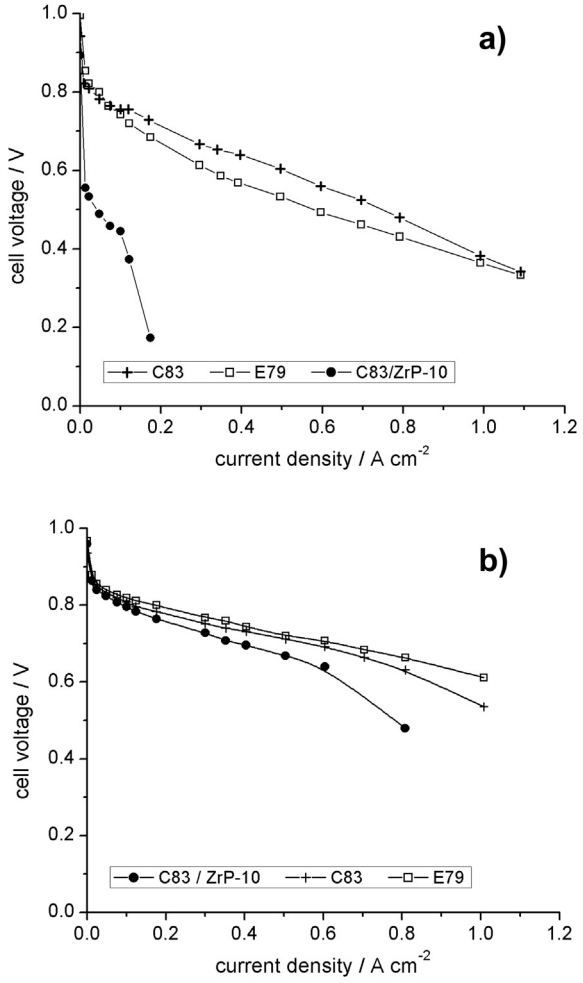

Fig. 8. Polarization curves for GDE MEAs based on the indicated membranes collected at (a) 80 °C, RHa = RHc = 30%, 1.5 bara and (b) 70 °C, RHa = RHc = 100%, 1.0 bara.

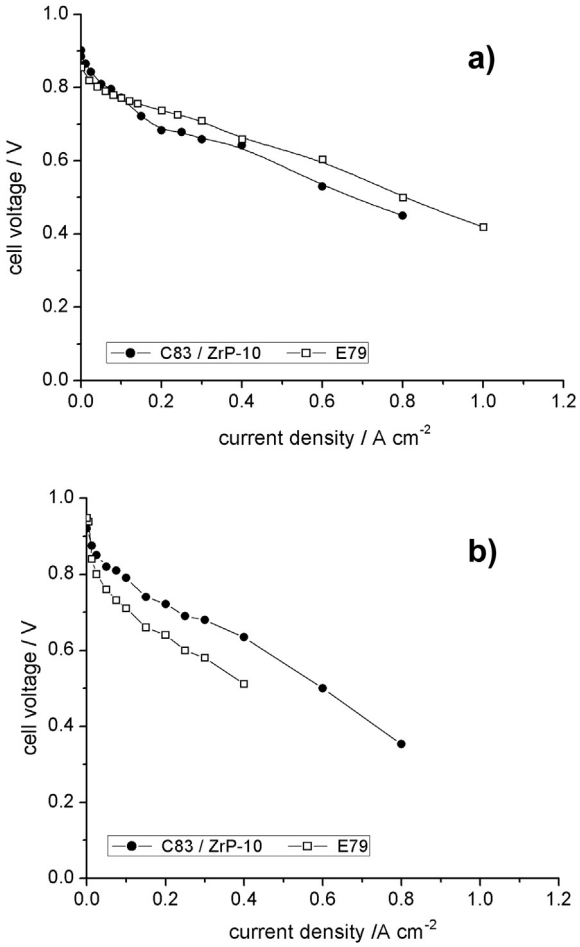

Fig. 9. Polarization curves for CCM MEAs based on the indicated membranes collected at (a) 80 °C, RHa = RHc = 30%, 1.5 bara and (b) 110 °C, RHa = 33.1%, RHc = 16.7%, 1.5 bara.

Table 3
Peak power densities for CCM MEAs based on C83/ZrP-10 composite membranes(RHa, RHc: relative humidity of the gas feeding anode and cathode, respectively; *P*: pressure).

T (°C)	%RHa/%RHc/P(bara)	Current density (A cm^{-2})	Peak power density (W cm^{-2})
80	30/30/1	0.8	0.36
100	46.8/23.7/1.5	0.6	0.30
110	33.1/16.7/1.5	0.6	0.28

as current starts circulating. The low performance of C83/ZrP-10 cannot be ascribed to membrane failure because when RH is increased to 100% the performance of the composite membrane approaches that of C83 and E79 (Fig. 8b).

Surprisingly, when measurements were performed with the CCM MEA, the performance of the composite membrane at 80 °C and 30% RH was only slightly lower than that of E79 (Fig. 9a). This kind of MEA was therefore used for tests at higher temperature. At 100 °C, the polarisation curves obtained with C83/ZrP-10 and E79 are nearly coincident (data not shown), while at 110 °C (with RHa = 33.1% and RHc = 16.7%) the composite membrane performs better than E79 (Fig. 9b). The peak power density of a CCM MEA based on C83/ZrP-10 lies in the range 0.36–0.28 W cm^{-2} at temperature between 80 and 110 °C without significant power decay between 100 and 110 °C (Table 3).

The lower fuel cell performance of E79 at 110 °C can hardly be ascribed to the bulk transport properties of the membrane since, at this temperature, E79 is more conductive than C83/ZrP-10 even at RH as low as 25%. Thus, the electrode-membrane interface is mainly responsible for the different performance of E79 and C83/ZrP-10. Accordingly, at 110 °C, the extrapolation to zero current of the linear region of the polarization curve of the E79 MEA lies below that of the C83/ZrP-10 MEA by about 60 mV thus indicating a higher activation overpotential for the E79 MEA.

4. Conclusion

Dispersion of nanosized ZrP within the matrix of an 830 EW SSC ionomer allowed to improve significantly the mechanical properties of the neat ionomeric membranes, both at ambient conditions and at 80 °C, while retaining to a large extent their ductile properties. Even with 10 wt% filler loading the conductivity of the composite membranes is as high as that of the neat ionomer and highly isotropic. Fuel cell tests performed with CCM type MEAs showed that the performance of the composite membrane incorporating 10 wt% ZrP is similar to that of the extruded E79 membrane at 80 °C and better than that at 110 °C. Therefore, as already reported for LSC ionomers [21], the fuel cell performance of membranes made of SSC ionomers as well benefits from the presence of nanosized ZrP for working temperature above 80 °C.

Acknowledgement

The EU-FP7 (FCH-JU) project “MAESTRO – MembranES for STationary application with Robust mechanical properties” (GA 256647), is gratefully acknowledged for co-funding this work.

References

[1] W. Groth, Fluorinated Ionomers, Elsevier, Oxford, 2011.
[2] B. Smitha, S. Sridhar, A.A. Khan, J. Membr. Sci. 259 (2005) 10–26.
[3] V. Arcella, C. Troglia, A. Ghielmi, Ind. Eng. Chem. Res. 44 (2005) 7646–7651.
[4] A. Ghielmi, P. Vaccarono, C. Troglia, V. Arcella, J. Power Sources 145 (2005) 108–115.
[5] K.D. Kreuer, M. Schuster, B. Obliers, O. Diat, U. Traub, A. Fuchs, U. Klock, S.J. Paddison, J. Maier, J. Power Sources 178 (2008) 499–509.
[6] M. Pica, A. Donnadio, M. Casciola, P. Cojocaru, L. Merlo, J. Mater. Chem. 22 (2012) 24902–24908.
[7] D.J. Jones, J. Roziere, in: W. Vielstick, H. Gasteiger, A. Lamm (Eds.), Handbook of Fuel Cells, Fundamentals, Technology and Applications, vol. 3, John Wiley & Sons, West Sussex, England, 2003.
[8] G. Alberti, M. Casciola, Annu. Rev. Mater. Res. 33 (2003) 129–154.
[9] F. Bauer, M. Willert-Porada, J. Membr. Sci. 233 (2004) 141–149.
[10] F. Bauer, M. Willert-Porada, Solid State Ionics 177 (2006) 2391–2396.
[11] G. Alberti, M. Casciola, A. Donnadio, R. Narducci, M. Pica, M. Sganappa, Desalination 199 (2006) 280–282.
[12] G. Alberti, M. Casciola, D. Capitani, A. Donnadio, R. Narducci, M. Pica, M. Sganappa, Electrochim. Acta 52 (2007) 8125–8132.
[13] M. Casciola, D. Capitani, A. Comite, A. Donnadio, V. Frittella, M. Pica, M. Sganappa, A. Varzi, Fuel Cells 3–4 (2008) 217–224.
[14] M. Casciola, G. Bagnasco, A. Donnadio, L. Micoli, M. Pica, M. Sganappa, M. Turco, Fuel Cells 9 (2009) 394–400.
[15] A.L. Moster, B.S. Mitchell, J. Appl. Polym. Sci. 111 (2009) 1144–1150.
[16] S. Subianto, M. Pica, M. Casciola, P. Cojocaru, L. Merlo, G. Hards, D.J. Jones, J. Power Sources 233 (2013) 216–230.
[17] M. Pica, A. Donnadio, D. Capitani, R. Vivani, E. Troni, M. Casciola, Inorg. Chem. 50 (2011) 11623–11630.
[18] M. Fujimura, T. Hashimoto, H. Kawai, Macromolecules 14 (1981) 1309–1315.
[19] M. Casciola, A. Donnadio, P. Sassi, J. Power Sources 235 (2013) 129–134.
[20] C.F. Nørgaard, U.G. Nielsen, E.M. Skou, Solid State Ionics 213 (2012) 76–82.
[21] C. Yang, S. Srinivasan, A.B. Bocarsly, S. Tulyani, J.B. Benziger, J. Membr. Sci. 237 (2004) 145–161.
[22] F. Bauer, M. Willert-Porada, Solid State Ionics 177 (2006) 2391.
[23] A. Clearfield, U. Costantino, in: G. Alberti, T. Bein (Eds.), Comprehensive Supramolecular Chemistry, vol. 7, Pergamon, 1996, pp. 107–149.
[24] M. Casciola, F. Marmottini, A. Peraio, Solid State Ionics 61 (1993) 125–129.
[25] G. Alberti, R. Narducci, M. Sganappa, J. Power Sources 178 (2008) 575–583.